8468 *Macromolecules* **2010**, *43*, 8468–8478
DOI: 10.1021/ma101814m

Macromolecules
ARTICLE

Jacketed Polymers with Dendritic Carbazole Side Groups and Their Applications in Blue Light-Emitting Diodes

Hao Jin, Yiding Xu, Zhihao Shen,* Dechun Zou,* Dan Wang, Wei Zhang, Xinghe Fan,* and Qifeng Zhou*

Beijing National Laboratory for Molecular Sciences, Key Laboratory of Polymer Chemistry and Physics of Ministry of Education, College of Chemistry and Molecular Engineering, Peking University, Beijing 100871, China

Received August 9, 2010; Revised Manuscript Received September 14, 2010

ABSTRACT: Styrene-based monomers with the first- and second-generation dendronized carbazoles were synthesized by a convergent strategy. Conventional free radical polymerizations were carried out to synthesize the dendronized jacketed polymers using these two monomers. The apparent molecular weights of the two polymers determined by gel permeation chromatography were 57 000 and 34 000 g/mol, respectively. The polymers had excellent thermal stability with their 5% weight loss temperatures all above 360 °C. Their photophysical properties in solutions and films were investigated. Different solvents had negligible effects on their UV−vis or photoluminescent (PL) spectra. A 10 nm blue shift of the emission peak was observed in the PL spectra of films compared with those of solutions. After the films were annealed, the emission peaks became narrower. X-ray diffraction techniques were utilized to examine the phase structures of the dendronized jacketed polymers. The first-generation polymer formed a hexatic columnar nematic phase, while the second-generation one exhibited a columnar nematic phase. This stiff main-chain conformation and the dendritic side-group structure could reduce the intramolecular interactions and aggregations of the carbazole side groups and prevent the formation of excimers, which would be beneficial to the optoelectronic properties. The two polymers showed similar electrochemical properties. Their HOMO levels were about −5.3 eV, which was quite close to that of PEDOT:PSS. Electroluminescent (EL) devices were fabricated in two configurations. A new emission peak was found in the EL spectra compared with the PL spectra. All the devices emitted blue lights and possessed low driving voltages. An introduction of an electron-transporting layer could greatly improve the device properties. The best device could reach a luminescence of 2195 cd/m^2, a current efficiency of 0.240 cd/A, and an external quantum efficiency of 0.353%.

Introduction

Organic light-emitting diodes (OLEDs) have attracted considerable attention for their applications in flat panel displays and lighting during the past decade because of their high electro-optical conversion efficiency, wide viewing angle, low driving voltage, and low cost.[1−4] Vacuum deposition techniques were applied to prepare the thin films to reduce the bias voltage of the devices and give a relatively high efficiency. The first polymer-based OLED (PLED) was fabricated in 1990,[5] and then numerous electroluminescent (EL) polymers with different chemical compositions and architectures were synthesized.[6−8] Compared with OLEDs from small molecules, PLEDs are able to fulfill different functions in one layer by incorporating charge-transporting groups and light-emitting groups in a single polymer chain, and thus the device structure will be much simpler. PLEDs are also considered as the most promising technology to realize flexible and large-area displays by wet-chemistry fabrication processes such as spin-coating or inkjet-printing.

Electroluminescent polymer materials can be divided into three groups, namely, main-chain type, side-chain type, and mixed type. Main-chain-type polymers possess a stiff conjugated main chain and are usually synthesized by condensation polymerizations. The conjugated main-chain structures make them much easier for carrier injection and transport,[9,10] and the stiff main chain is also of benefit to inhibit the aggregation of light-emitting groups and prevent fluorescence quenching and formation of excimers. However, their molecular weights (MWs) are difficult to control during polymerization, and the MW distributions are usually broad. In addition, conjugated polymers also suffer from the poor solubility in organic solvents. Compared with main-chain-type polymers, side-chain-type polymers can be synthesized through free radical polymerization and usually possess a vinyl main chain.[11,12] Different polymers can be readily synthesized by changing the covalently bonded functional side groups to adjust the light-emitting wavelength and device properties.[13] Recently, controlled/living polymerization techniques, such as nitroxide-mediated polymerizations (NMP)[14,15] and reversible addition−fragmentation transfer (RAFT) polymerizations,[16] are more and more frequently utilized to synthesize these polymers, with their structure parameters exactly controlled. And electroluminescent polymers with complex architectures can be obtained. Mixed-type electroluminescent copolymers have also been reported.[17] The copolymer chains are composed of two blocks, one being a side-chain type and the other a main-chain type. Such copolymers provide an excellent model to investigate the relationship between the phase structure and optoelectronic properties of the electroluminescent polymers.

Mesogen-jacketed liquid crystalline polymers (MJLCPs) refer to a class of side-chain liquid crystalline polymers (SCLCPs) in which the side-chain mesogens are side-on attached with a very

*To whom correspondence should be addressed. E-mail: (X.F.) fanxh@pku.edu.cn; (Z.S.) zshen@pku.edu.cn; (D.Z.) dczou@pku.edu.cn; (Q.Z) qfzhou@pku.edu.cn.

 Published on Web 09/30/2010

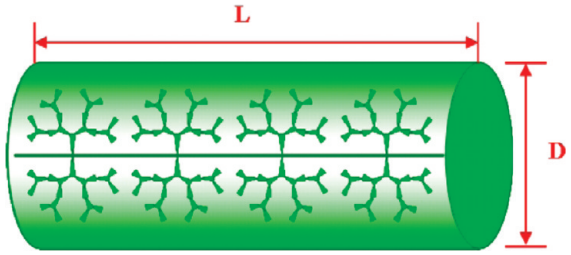

Figure 1. Cylindrical structure of the dendronized jacketed polymer.

short spacer or without any spacer at all.[18,19] The main chain was forced to take an extended chain conformation because of the steric hindrance exerted by the highly populated bulky, rigid side groups. Although MJLCPs, as SCLCPs, can be easily synthesized by conventional and controlled/living free radical polymerizations, they behave like main-chain liquid crystalline polymers in that the whole polymer chain serves as a supramolecular mesogen. In the past two decades, systematic research on the structure−property relationships for MJLCPs with different side groups has been done.[20,21] Recently, the functionalization of this system has been researched. It has been proven that introducing bulky, rigid side groups to form electroluminescent jacketed polymers was helpful in inhibiting the aggregation of functional groups, and some jacketed polymers can be used for electrophosphorescent systems as host materials.[22−26]

Dendronized polymers[27,28] are special polymer brushes with a dendronized side group in each repeating unit. When the generation of the dendrons is high enough, the steric hindrance produced by the huge side groups will force the main chain to exhibit a stiff conformation similar to MJLCPs.[29−33] Usually, there are three strategies to construct a dendronized polymer, namely, "graft through", "graft from", and "graft onto".[34−36] Among these three methods, the "graft through" strategy is also called the macromonomer strategy, which means the polymerization of a macromonomer with a dendrimer structure.[33] This method can control the structure more precisely, and each repeating unit can be introduced with dendrons having the same structures and generations, avoiding uneven, uncontrolled generations or distributions of dendrons on the main chain in the other two strategies. However, the huge steric hindrance usually leads to a low conversion of the macromonomers, and the removal of the unreacted monomers is tedious. Several reports on main-chain-type dendronized electroluminescent polymers have demonstrated the importance of the dendritic structure for suppressing aggregations and fluorescence quenching.[37,38] However, little work has been done on vinyl dendronized electroluminescent polymers.

Carbazoles and their derivatives have been used widely as hole-transporting materials and emitting materials.[39,40] In this contribution, dendritic carbazole side groups were introduced by the "graft through" method into MJLCPs for the first time. The phase structures and optoelectronic properties of the resulting polymers were investigated. Compared with traditional side-chain polymers, these polymers were expected to have the advantage of distributing carbazoles on the surface of the rod-like polymer chain, and thus the electroluminescent functions of carbazoles could be utilized sufficiently. In addition, the rigid rod-like polymer chain might inhibit the aggregation of the carbazoles and provide a continuous channel for transporting holes. From the viewpoint of molecular engineering, the length (L) of the stiff, cylindrical chain could be controlled by the degree of polymerization, and the diameter (D) could be adjusted by the number of generations of carbazole side groups (Figure 1). Therefore, the optoelectronic properties of the polymers could be tailored.

Experimental Details

Materials. 2,2′-Azobis(isobutyronitrile) (AIBN) was recrystallized from ethanol. Chlorobenzene was washed with sulfuric acid and then distilled under reduced pressure. All the other reagents were used as received.

Characterization. ^{1}H NMR spectra were recorded on a Mercury plus 300 MHz or Bruker 400 MHz using deuterated chloroform ($CDCl_3$) or deuterated dimethyl sulfoxide (DMSO-d) as solvents at room temperature. The chemical shifts were reported in ppm with tetramethylsilane (TMS) as the internal standard. Mass spectra were recorded on a Bruker Apex IV FTMS or Autoflex III MALDI−TOF spectrometer. Elemental analyses were carried out on an Elementar Vario EL (Germany). Gel permeation chromatographic (GPC) measurements were carried out at 35 °C on a Waters 2410 instrument equipped with three Waters μ-Styragel columns (103, 104, and 105 Å) in series, using tetrahydrofuran (THF) as the eluent at a flow rate of 1.0 mL/min. All of the GPC data were calibrated with linear polystyrene standards.

Thermogravimetric analysis (TGA) was performed with a Q600 SDT instrument at a heating rate of 20 °C/min in a nitrogen atmosphere. Differential scanning calorimetry (DSC, PerkinElmer Pyris I with a mechanical refrigerator) was utilized to study the glass transitions of the polymers. A typical DSC sample size was about 2 mg. The samples were encapsulated in hermetically sealed aluminum pans, and the pan weights were kept constant. The temperatures and heat flow scales at different cooling and heating rates were calibrated using standard materials such as indium and benzoic acid. The glass transition temperatures (T_g's) were obtained from the second heating curves.

Absorption spectra were measured with a Jasco V-550 spectrophotometer, and photoluminescent (PL) spectra were obtained using a Hitachi F-4500 fluorescence spectrophotometer. The electrochemical properties were measured using a voltammetric analyzer (CHI630C from Shanghai Chenhua Instrument Company, China) at a scanning rate of 100 mV/s at room temperature. A three-electrode system was used. A polymer-coated carbon electrode was used as the working electrode, Ag/AgCl electrode as reference electrode, and platinum wire electrode as auxiliary electrode, supported with 0.1 M $(n\text{-Bu})_4\text{-NClO}_4$ in acetonitrile. A solution of ferrocene (FOC) (1×10^{-3} M in acetonitrile) was tested by the same method to obtain the half-wave potential ($U_{1/2,\mathrm{FOC}}$) of FOC/FOC$^+$. The energy levels of polymers were calculated using the FOC value of −4.8 eV with respect to vacuum level, which was defined as zero. Therefore, the HOMO levels of the polymers could be calculated by the equation $E_{\mathrm{HOMO}} = -e[U_{\mathrm{onset(ox)}} + (4.8\ \mathrm{V} - U_{1/2,\mathrm{FOC}})]$ and the LUMO levels could be estimated by the equation $E_{\mathrm{LUMO}} = -e[U_{\mathrm{onset(red)}} + (4.8\ \mathrm{V} - U_{1/2,\mathrm{FOC}})]$.

The phase structures of the samples at different temperatures were studied by one-dimensional (1D) and two-dimensional (2D) wide-angle X-ray diffraction (WAXD) experiments. 1D WAXD experiments were performed on a Philips X'Pert Pro diffractometer with a 3-kW ceramic tube as the X-ray source (Cu Kα) and an X'celerator detector. Silicon powder and silver behenate were used to calibrate the reflection peak positions at $2\theta > 15°$ and $2\theta < 10°$, respectively. A hot stage (Paar Physica YCU 100) was utilized to study the phase structure evolutions with varing temperature. The heating and cooling rates in all WAXD experiments were 10 °C/min. 2D WAXD experiments were performed on a Bruker D8Discover diffractometer with GADDS as a 2D detector. Silicon powder and silver behenate were used as standards again. The 2D diffraction patterns were recorded in a transmission mode at room temperature. The oriented samples were prepared by mechanically shearing the films at 120 °C. The sheared film was positioned so that the mechanical shearing direction was either perpendicular or parallel to the point-focused X-ray beam. For both the 1D and 2D diffractions, the background scattering was recorded and subtracted from the sample patterns.

Device Fabrication and Characterization. The patterned indium tin oxide (ITO) substrate was cleaned by detergents, deionized water, acetone, and ethanol, in sequence, and then treated with UV−ozone for about 25 min. Poly(3,4-ethylenedioxythiophene):poly(styrenesulfonate) (PEDOT:PSS) was spin-coated on the precleaned ITO substrate and dried in air at 120 °C for 2 h. Then the polymer was spin-coated from a chlorobenzene solution (10 mg/mL) through a 0.45-μm Teflon filter. The thickness of the spin-coated film was controlled by the spinning speed. The coated ITO substrate was transferred into a deposition chamber with a base pressure of 6×10^{-4} Pa. 1,3,5-Tris(1-phenyl-1*H*-benzimidazol-2-yl)benzene (TPBI), 8-hydroxyquinoline aluminum (AlQ), and metal layers were deposited on top of the polymer layer. The emitting area was 2×2 mm^2. The EL spectra were measured with a spectrofluorometer FP-6200 (JASCO). A source-measure unit R6145 (Advantest), multimeter 2000 (Keithley), and luminance meter LS-110 (Minolta) were used for $I-V-L$ measurements. Relative luminance was directly detected by using a multifunctional optical meter 1835-C (Newport). All the fabrication and characterization of the devices were performed in air and at room temperature without protective encapsulation.

Synthesis. Syntheses of the monomers and polymers were carried out following the routes outlined in Scheme 1.

Synthesis of 5-(Benzyloxy)isophthalic Acid (1). After dissolving 5-hydroxyisophthalic acid (5.0 g, 27.5 mmol) in methanol (25 mL), concentrated sulfuric acid (3.2 mL) was added dropwise. The reaction mixture was refluxed for 5 h. After the mixture was cooled, methanol was removed by a rotary evaporator to give a white powder, which was dissolved in ethyl acetate (100 mL) and washed with water (100 mL × 3), a saturated sodium bicarbonate solution (100 mL × 3), and water (100 mL). Then the organic layer was dried with anhydrous magnesium sulfate for 30 min, and the solvent was evaporated. The residue was dissolved in acetone (100 mL), with the addition of bromomethylbenzene (5.6 g, 33.0 mmol) and anhydrous potassium carbonate (7.0 g, 50.0 mmol). The mixture was refluxed for 2 h, and the hot solution was filtered. The filtrate was concentrated by a rotary evaporator to give a white powder, which was dissolved in THF (50 mL), and a sodium hydroxide solution (5 M, 25 mL) was added. Then the reaction temperature was increased to 60 °C. After 8 h, the mixture was poured into 800 mL of water and acidified with hydrochloride acid to give a white precipitate. Filtered, washed with water, and dried in a vacuum oven, the target product was obtained as a white powder (5.6 g, 20.6 mmol) in 75% yield. ^{1}H NMR (300 MHz, DMSO-*d*, δ, ppm): 5.25 (s, 2H, $-OCH_2$), 7.33−7.57 (m, 5H, Ar−H), 7.76 (s, 2H, Ar−H), 8.11 (s, 1H, Ar−H), 13.35 (s, 2H, −COOH). Anal. Calcd for $C_{15}H_{15}ON$: C, 66.17; H 4.44. Found: C, 66.36; H, 4.53.

Synthesis of 3-(9*H*-Carbazol-9-yl)propan-1-ol (2). To a magnetically stirred solution of 3-bromopropan-1-ol (10.0 g, 71.8 mmol) in *N*,*N*′-dimethylformamide (DMF, 30 mL) was added 3,4-dihydro-2*H*-pyran (12.1 g, 143.5 mmol) dropwise, and then the solution was stirred at room temperature. After 1 h, carbazole (6.0 g, 35.9 mmol) and sodium hydroxide (2.9 g, 71.8 mmol) were added to the solution, and the temperature was increased to 90 °C. The mixture was stirred for 5 h. After the hot solution was filtered, the filtrate cake was washed by DMF three times, The filtrate was added with methanol (30 mL) and 4-methylbenzenesulfonic acid (3.4 g, 17.9 mmol), and the reaction mixture was stirred overnight at 50 °C and then concentrated at 65 °C under reduced pressure. The crude product was dissolved in ethanol and precipitated in a large amount of water. After the precipitate was filtered and dried, the pure product was obtained by silica gel column chromatography (CH_2Cl_2:petroleum ether = 3:1) as a white solid (5.1 g, 22.6 mmol) in 63% yield. ^{1}H NMR (300 MHz, $CDCl_3$, δ, ppm): 2.06−2.18 (m, 2H, $HOCH_2CH_2$), 3.59−3.65 (t, 2H, $HOCH_2$), 4.44.-4.51 (t, 2H, CH_2N), 7.19−7.29 (m, 2H, Ar−H), 7.46−7.48 (m, 4H, Ar−H), 8.08−8.12 (m, 2H, Ar−H). Anal. Calcd for $C_{15}H_{15}ON$: C, 79.97; H, 6.71; N, 6.22. Found: C, 80.00; H, 6.76; N, 6.24.

Synthesis of Bis[3-(9*H*-carbazol-9-yl)propyl]-5-(benzyloxy)-isophthalate (3). 5-(Benzyloxy)isophthalic acid (3.8 g, 14.0 mmol), 3-(9*H*-carbazol-9-yl)-propan-1-ol (7.2 g, 32 0.0 mmol), *N*,*N*′-dicyclohexylcarbodiimide (DCC, 7.2 g, 35.0 mmol), and 4-(dimethylamino)pyridine (DMAP, 0.5 g, 4.2 mmol) were added into 200 mL of CH_2Cl_2. The mixture was stirred overnight at room temperature and filtered. The filtrate was concentrated by a rotary evaporator, and the residue was washed with acetone first and then purified through a silica gel column (CH_2Cl_2: petroleum ether = 3:2) to afford the pure product as a white solid (6.1 g, 8.9 mmol) in 64% yield. ^{1}H NMR (300 MHz, $CDCl_3$, δ, ppm): 2.35−2.41 (m, 4H, $CH_2CH_2CH_2$), 4.32−4.38 (t, 4H, CH_2N), 4.47−4.53 (t, 4H, $COOCH_2$), 5.16 (s, 2H, OCH_2), 7.16−7.26 (m, 4H, Ar−H), 7.35−7.50 (m, 13H, Ar−H), 7.80 (s, 2H, Ar−H), 8.05−8.09 (d, 4H, Ar−H), 8.31−8.32 (t, 1H, Ar−H). Anal. Calcd for $C_{45}H_{38}O_5N_2$: C, 78.70; H, 5.58; N, 4.08. Found: C, 78.76; H, 5.80; N, 4.13.

Synthesis of Bis[3-(9*H*-carbazol-9-yl)propyl]-5-(3-hydroxy-propoxy)isophthalate (4). Bis[3-(9*H*-carbazol-9-yl)propyl]-5-(benzyloxy)isophthalate (17.0 g, 24.8 mmol) was dissolved in THF (250 mL), and Pa/C catalyst (3.0 g) was added. The mixture was stirred under a hydrogen atmosphere at room temperature for 8 h. Then the mixture was filtered through Celite, and the filtrate was concentrated to obtain a white solid, which was dissolved in acetone (250 mL), followed by the addition of 3-bromopropan-1-ol (6.9 g, 49.5 mmol), anhydrous potassium carbonate (6.8 g 49.5 mmol), and potassium iodide (1.2 g, 7.2 mmol). The mixture was refluxed for 8 h, and the hot solution was filtered. The filtrate was concentrated by a rotary evaporator, and the residue was washed with ethanol to give the crude product. The pure product was obtained through a silica gel column (ethyl acetate:petroleum ether = 1:1) as a white powder (15.6 g, 23.8 mmol) in 95% yield. ^{1}H NMR (300 MHz, $CDCl_3$, δ, ppm): 2.06−2.15 (m, 2H, $HOCH_2CH_2$), 2.29−2.42 (m, 4H, $COOCH_2CH_2$), 3.89−3.93 (t, 2H, $HOCH_2$), 4.19.-4.23 (t, 2H, OCH_2), 4.33−4.37 (t, 4H, CH_2N), 4.48−4.52 (t, 4H, $COOCH_2$), 7.18−7.25 (m, 4H, Ar−H), 7.39−7.43 (m, 8H, Ar−H), 7.73−7.74 (d, 2H, Ar−H), 8.06−8.09 (d, 4H, Ar−H), 8.31−8.32 (t, 1H, Ar−H). Anal. Calcd for $C_{41}H_{38}O_6N_2$: C, 75.21; H, 5.85; N, 4.28. Found: C, 75.21; H, 5.91; N, 4.26.

Synthesis of Monomer 1. Bis[3-(9*H*-carbazol-9-yl)propyl]-5-(3-hydroxypropoxy)isophthalate (5.4 g, 8.3 mmol), 2-vinylterephthalic acid (0.8 g, 4.1 mmol), DCC (1.9 g, 9.1 mmol), and DMAP (0.1 g, 0.9 mmol) were added into 100 mL of CH_2Cl_2 simultaneously. The mixture was stirred overnight at room temperature and filtered. The filtrate was concentrated by a rotary evaporator, and the residue was purified through a silica gel column using CH_2Cl_2 as the eluent. The target **monomer 1** was obtained as a white solid (3.7 g, 2.5 mmol) in 61% yield. ^{1}H NMR (400 MHz, $CDCl_3$, δ, ppm): 2.29−2.40 (m, 12H, $CH_2CH_2CH_2$), 4.18−4.22 (m, 4H, OCH_2), 4.32−4.35 (t, 8H, CH_2N), 4.47−4.50 (t, 8H, $COOCH_2$), 4.54−4.59 (q, 4H, $COOCH_2$), 5.34−5.37 (d, 1H, $=CH_2$), 5.67−5.71 (d, 1H, $=CH_2$), 7.17−7.25 (m, 8H, Ar−H), 7.33−7.43 (m, 17H, Ar−H, CH=), 7.72 (s, 4H, Ar−H), 7.86−7.93 (m, 2H, Ar−H), 8.05−8.07 (d, 8H, Ar−H), 8.19 (s, 1H, Ar−H), 8.30 (s, 2H, Ar−H). MS (HR-ESI): m/z 1482.60299 $[M + NH_4]^+$. Anal. Calcd for $C_{92}H_{80}O_{14}N_4$: C, 75.39; H, 5.50; N, 3.82. Found: C, 75.11; H, 5.68; N, 4.00.

Synthesis of BnCbzG2 (5). 5-(Benzyloxy)isophthalic acid (1.1 g, 4.0 mmol), bis[3-(9*H*-carbazol-9-yl)-propyl]-5-(3-hydroxy-propoxy)isophthalate (5.3 g, 8.1 mmol), DCC (1.9 g, 9.2 mmol), and DMAP (0.1 g, 0.8 mmol) were added into CH_2Cl_2 (100 mL). The mixture was stirred at room temperature for 9 h and filtered. The filtrate was concentrated by a rotary evaporator, and the residue was purified through a silica gel column (CH_2Cl_2:ethyl acetate = 100:1) to give the pure product as a white solid (3.9 g, 2.5 mmol) in 62% yield. ^{1}H NMR (400 MHz, $CDCl_3$,

Scheme 1. Syntheses of the First- and Second-Generation Monomers and Polymers

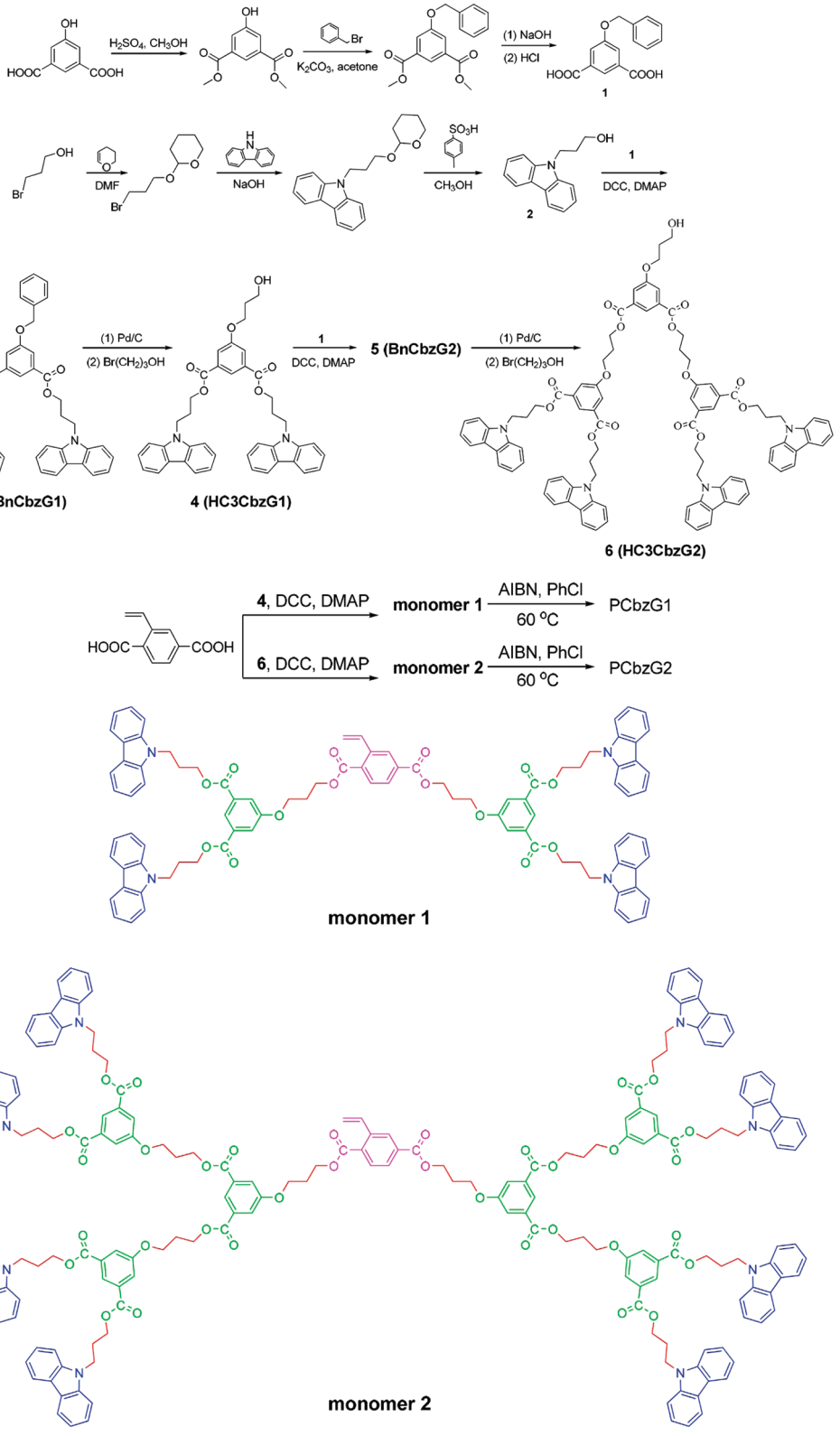

δ, ppm): 2.29−2.38 (m, 12H, $CH_2CH_2CH_2$), 4.16−4.19 (t, 4H, OCH_2), 4.30−4.33 (t, 8H, CH_2N), 4.45−4.48 (t, 8H, $COOCH_2$), 4.53−4.57 (t, 4H, $COOCH_2$), 5.03 (s, 2H, OCH_2), 7.16−7.20 (m, 8H, Ar−H), 7.33−7.42 (m, 21H, Ar−H), 7.69−7.70 (d, 4H, Ar−H), 7.77−7.78 (d, 2H, Ar−H), 8.04−8.06 (d, 8H, Ar−H), 8.28−8.29 (m, 3H, Ar−H). MS (LR-ESI): m/z 1546.6 $[M + H]^+$. Anal. Calcd for $C_{97}H_{84}O_{15}N_4$: C, 75.37; H, 5.48; N, 3.62. Found: C, 75.50; H, 5.74; N, 3.63.

Synthesis of HC3CbzG2 (6). To a solution of BnCbzG2 (11.0 g, 7.1 mmol) in THF (250 mL) was added Pa/C catalyst (2.5 g). The mixture was stirred under a hydrogen atmosphere at room temperature for 10 h and then filtered through Celite. The filtrate was concentrated to obtain a white solid, which was dissolved in acetone (250 mL), followed by the addition of 3-bromopropan-1-ol (2.8 g, 19.8 mmol), anhydrous potassium carbonate (2.7 g 19.8 mmol), and potassium iodide (0.3 g,

1.6 mmol). The mixture was refluxed for 7 h, and the hot solution was filtered. The filtrate was concentrated by a rotary evaporator, and the residue was washed with ethanol to give the crude product. The pure product was obtained through a silica gel column (ethyl acetate:petroleum ether = 2:1) as a white powder (10.2 g, 6.7 mmol) in 94% yield. ^{1}H NMR (400 MHz, $CDCl_3$, δ, ppm): 1.94−2.00 (m, 2H, $HOCH_2CH_2$), 2.29−2.39 (m, 12H, $CH_2CH_2CH_2$), 3.76−3.79 (t, 2H, $HOCH_2$), 4.07−4.10 (t, 2H, OCH_2), 4.17−4.20 (t, 4H, OCH_2), 4.31−4.34 (t, 8H, CH_2N), 4.45−4.49 (t, 8H), 4.54−4.57 (t, 4H, $COOCH_2$), 7.11−7.21 (m, 8H, $COOCH_2$), 7.37−7.42 (m, 16H, Ar−H), 7.69−7.70 (d, 6H, Ar−H), 8.04−8.06 (d, 8H, Ar−H), 8.26−8.29 (m, 3H, Ar−H). MS (LR-ESI): m/z 1513.6 $[M + H]^+$. Anal. Calcd for $C_{93}H_{84}O_{16}N_4$: C, 73.79; H, 5.59; N, 3.70. Found: C, 73.55; H, 5.75; N, 3.65.

Synthesis of Monomer 2. HC3CbzG2 (5.5 g, 3.6 mmol), 2-vinylterephthalic acid (0.3 g, 1.8 mmol), DCC (0.9 g, 4.6 mmol), and DMAP (0.1 g, 0.9 mmol) were added into CH_2Cl_2 (150 mL) simultaneously. The mixture was stirred overnight at room temperature and filtered. The filtrate was concentrated by a rotary evaporator, and the residue was purified through a silica gel column (CH_2Cl_2:ethyl acetate = 30:1) to give the pure product as a white solid (2.8 g, 0.9 mmol) in 49% yield. ^{1}H NMR (400 MHz, $CDCl_3$, δ, ppm): 2.28−2.37 (m, 28H, $CH_2CH_2CH_2$), 4.08−4.18 (m, 12H, OCH_2), 4.30−4.33 (t, 16H, CH_2N), 4.44−4.47 (t, 20H, $COOCH_2$), 4.53−4.56 (t, 8H, $COOCH_2$), 5.33−5.35 (d, 1H, $=CH_2$), 5.65−5.69 (d, 1H, $=CH_2$), 7.14−7.21 (m, 16H, Ar−H), 7.30−7.41 (m, 33H, Ar−H, =CH), 7.68−7.70 (m, 12H, Ar−H), 7.82−7.89 (m, 2H, Ar−H), 8.03−8.05 (d, 16H, Ar−H), 8.15 (s, 1H, Ar−H), 8.26−8.28 (m, 6H, Ar−H). MS (MALDI−TOF): m/z 3204.5 $[M + Na]^+$. Anal. Calcd for $C_{196}H_{172}O_{34}N_8$: C, 73.95; H, 5.45; N, 3.52. Found: C, 71.30; H, 5.40; N, 3.36.

Polymerization of Monomer 1. Monomer 1 (100 mg), chlorobenzene (864 mg), and 37 μL of chlorobenzene solution containing 0.22 mg of AIBN were transferred into a precleaned glass tube. After three freeze−pump−thaw cycles, the tube was sealed off under vacuum. Polymerization was performed at 60 °C for 20 h, and the mixture was quenched in liquid nitrogen. Then the tube was opened, and the solution was diluted with 5 mL of THF. The target polymer was precipitated in 200 mL of acetone. To ensure that the unreacted monomers was eliminated, the precipitation process was repeated three times. By filtration, the target polymer PCbzG1 was obtained as a white solid in 75% yield.

Polymerization of Monomer 2. Monomer 2 (300 mg), chlorobenzene (1.14 g), and 52 μL of chlorobenzene solution containing 0.31 mg of AIBN were transferred into a precleaned glass tube. Polymerization was carried out similarly compared to that for synthesizing PCbzG1. The target polymer PCbzG2 was obtained as a white solid in 40% yield.

Results and Discussion

Synthesis and Characterization of Monomers and Polymers. As mentioned before, the "graft through" strategy can control the chemical structure of dendronized polymers more precisely. We chose to synthesize the dendritic macromonomers first and then perform the polymerizations as illustrated in Scheme 1. In this way, a dendronized polymer with the same dendritic side groups in each repeating unit could be obtained. There are usually two ways to synthesize a dendritic molecule.[41] One is the divergent method. A core is synthesized first in this method, and then the dendritic shells grow from the core sequentially to form different generations of molecules. The other way is the convergent method, which begins with the synthesis of different generations of dendritic shells, followed by a reaction with the core. In the present work, the core had a styrene structure for the polymerization in the final step. Therefore, the convergent method was utilized to prevent side reactions of the double bond in the long synthetic routes. To ensure high yields of the monomers, highly efficient reactions, such as Williamson etherification, DCC esterification, and catalytic hydrogenation reactions, were chosen. The monomer structures were confirmed by ^{1}H NMR spectra, mass spectra, and elemental analysis.

Table 1. Molecular Weights and Thermal Properties of the Polymers

polymer	yield (%)	M_n (g/mol)[a]	M_w/M_n[a]	T_d (°C)[b]	T_g (°C)[c]
PCbzG1	75	57 000	1.89	364	87
PCbzG2	40	34 000	1.55	382	86

[a] Determined by GPC in THF using polystyrene standards. [b] 5% weight loss temperature evaluated by TGA under a nitrogen atmosphere at a heating rate of 20 °C/min. [c] Evaluated by DSC during the second heating cycle at a rate of 20 °C/min.

PCbzG1 and PCbzG2 were synthesized under the same conditions by conventional free radical polymerization in solution using chlorobenzene as the solvent. The number-average molecular weight (M_n), the molecular weight distribution, and the thermal properties of the polymers are summarized in Table 1. Although the two polymerizations were carried out under the same conditions, with the same ratio (50:1) of monomer concentration to initiator concentration, monomer weight concentration (10%), solvent, temperature, and reaction time, they showed different polymerization results. The second-generation monomer had a larger molecular weight than the first-generation one. However, PCbzG2 had a lower M_n and a lower monomer conversion compared with PCbzG1, which was probably due to a lower concentration of the double bond and a larger steric hindrance of **monomer 2**. To reduce the steric hindrance in the polymerization and improve the reactivity of the monomers, a short spacer had been introduced between the core and the dendritic shells in both monomers. However, **monomer 2** still had a much stronger steric hindrance effect than **monomer 1**. Excellent solubility was of great importance for dendronized polymers, especially for OLED applications. Therefore, we constructed the monomers with ester connections, which was also beneficial to the film-forming ability in a wet-processing technology. The polymers obtained could be readily dissolved in common organic solvents, such as THF, chlorobenzene, CH_2Cl_2, $CHCl_3$, ethyl acetate, DMF, etc. In addition, the dendronized **monomer 1** and **monomer 2** could be readily dissolved in acetone and thus could be removed easily after the polymerization.

The glass transition temperatures of the polymers were approximately 85 °C. Both polymers exhibited 5% weight loss temperatures above 360 °C, and the temperature of PCbzG2 was about 20 °C higher than that of PCbzG1. No weight loss was found at low temperatures. The excellent thermal properties indicated that these kind of dendronized polymers were suitable for device fabrication.

Photophysical Properties. The photophysical properties of the two polymers were investigated in different solvents and films. The absorption and emission data are summarized in Table 2. The UV−vis absorption spectra of the polymers are shown in Figure 2. All the spectra showed similar absorption bands with peaks at about 262 and 295 nm, which were due to the $\pi-\pi^*$ transition of the carbazole moiety.[42] The minor difference in the absorbing wavelength suggested that different solvents or different states had little influence on the ground-state electronic transitions.

The PL spectra were obtained after excitation at 280 nm. The spectra of the two polymers in THF and $CHCl_3$ all showed a single emission at approximately 440 nm

Table 2. UV−Vis and PL Spectra Data in Solutions and Films

	in THF[a]		in $CHCl_3$[a]		in films		
polymer	UV (nm)	PL (nm)[b]	UV (nm)	PL (nm)[b]	UV (nm)[c]	PL (nm)[b,c]	PL (nm)[b,d]
PCbzG1	261, 295	439	263, 295	440	262, 297	429	430
PCbzG2	262, 295	437	263, 295	441	262, 297	431	415

[a] 0.1 mg/mL. [b] Excitation wavelength was 280 nm. [c] Films were cast from THF solutions and dried at room temperature. [d] Films were cast from THF solutions, dried at room temperature, and then annealed at 120 °C for 2 h.

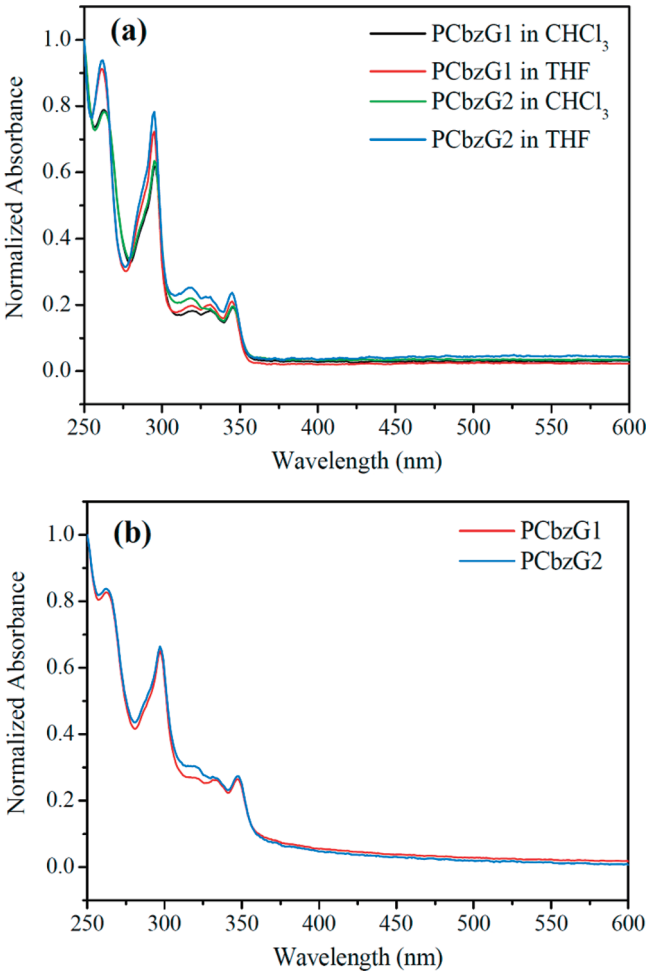

Figure 2. Normalized UV−vis absorption spectra in solutions (a) and films (b).

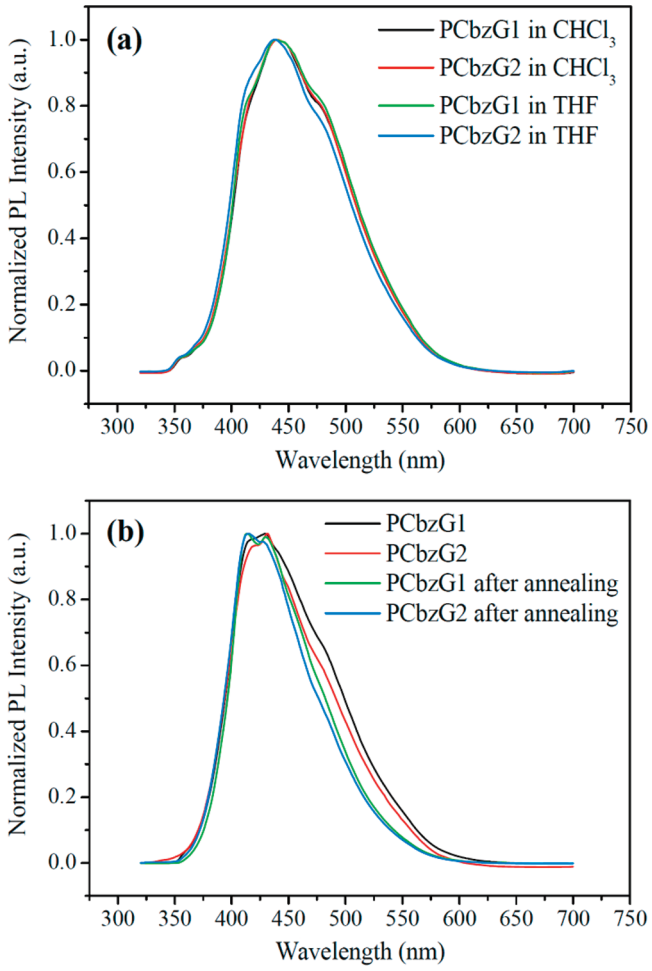

Figure 3. Normalized PL spectra in solutions (a) and films (b).

(Figure 3a). No obvious differences were found between the spectra of the two polymers in different solvents, which also supported the conclusions that different solvents played a minor role in the photophysical behavior and that similar excitation structures and radiative transition processes existed in the two polymers. Interestingly, we found that the PL emission in films (Figure 3b) showed different characteristics compared with that in solutions. The films were prepared from the corresponding polymer solutions (10 mg/mL) by spin-coating on a quartz plate and then dried at room temperature. The maximum emission peaks in the spectra of the two polymer films were both ~430 nm, which blue-shifted 10 nm compared with those of the polymer solutions. Since no additional conjugated structures were available in the polymers, the blue shift of the PL spectra could be due to the rearrangements of the polymer chains in films. After the polymer films were annealed at 120 °C for 2 h, the emission spectra became even narrower, and no excimer emissions were found at longer wavelengths, which further indicated the transition of the polymer conformation and that this transition would not lead to the aggregation of the dendritic functional groups.

Phase Structures of the Dendronized Polymers. In order to investigate the underlying reason for the changes in the PL spectra in films and study the phase behaviors of the two new jacketed polymers, 1D and 2D WAXD experiments were carried out to determine their phase structures. About 30 mg of sample was dissolved into 2 mL of THF, and then the solution was cast onto a cleaned copper substrate. The solvent was evaporated at room temperature, and finally the film was annealed at 120 °C for 48 h before testing. Figure 4 shows the 1D WAXD patterns of the first- and second-generation dendronized polymers during the first heating and the subsequent cooling processes. For PCbzG1, a sharp diffraction peak with a 2θ value of 3.04° was observed at 40 °C, indicating the existence of an ordered packing. With increasing temperature, the intensity of the peak increased. And the intensity decreased during cooling. Because of the limited number of diffractions, it was difficult to determine the exact phase structure from the 1D WAXD results alone. The phase structure could be a columnar nematic

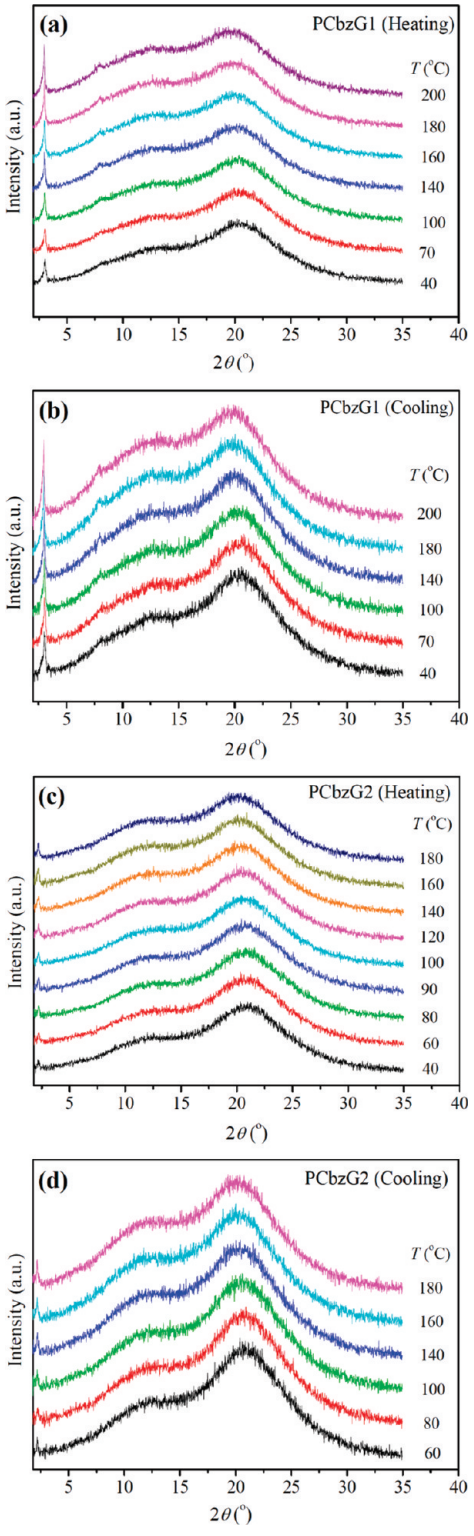

Figure 4. 1D WAXD patterns of PCbzG1 (a and b) and PCbzG2 (c and d) during their first heating and the subsequent cooling processes.

(Φ_N) phase with a *d*-spacing of 2.90 nm, although it was difficult to confirm by polarized light microscopy due to the rigid nature of the sample. A weaker diffraction peak at ~7.90° with a *d*-spacing of 1.12 nm was also found during the two processes. It was also difficult to judge the origin of this peak from the 1D patterns. For PCbzG2, only one diffraction peak could be found in the low-angle region, and the diffraction angel was 2.17° with a *d*-spacing of 4.07 nm. The intensity of this peak was much weaker than that of the low-angle peak for PCbzG1, probably due to the lower MW of PCbzG2 as the phase behavior of MJLCPs are MW-dependent.[21] However, the LC phase of PCbzG2 was less ordered than that of PCbzG1, based on the much less intense low-angle diffraction peak in parts c and d of Figure 4. In addition to the regular amorphous halo at ~20°, a second amorphous halo at ~12° was always present in Figure 4a–d, and it was also found in the diffraction patterns of the monomers. Therefore, it might result from the short-range arrangement of the dendritic carbazole side groups.

2D WAXD was also utilized to determine the phase structures of the two polymers. The samples were annealed at 170 °C and then sheared at the same temperature. Figure 5 shows the diffraction patterns with the X-ray incident beam perpendicular and parallel to the shear direction. As shown in Figure 5, the two polymers showed different diffraction patterns. For PCbzG1, when the X-ray incident beam was parallel to the shear direction (Figure 5a), six diffraction arcs were observed in the low-angle region. The azimuthal scan of the low-angle diffraction arcs exhibited six maxima which were separated by 60° from the adjacent ones (Figure 5c), indicating a 6-fold symmetry. On the other hand, the pattern obtained with the X-ray incident beam perpendicular (along *Y* direction) to the shear direction showed a pair of low-angle arcs on the meridian along with a diffuse high-angle halo concentrated on the equator (Figure 5b). These two patterns confirmed the existence of a columnar phase, actually a hexatic columnar nematic phase (Φ_{HN}, Figure 6a), instead of a smectic phase. From the low-angle *d*-spacing of 2.90 nm, which was consistent with the 1D WAXD results, the diameter of the polymer columns was calculated to be 3.35 nm. This value was close to the simulated molecular length (2.81 nm) of **monomer 1**, and the difference could be attributed to the loose packing of the nematic phase. In addition, the weak diffraction at a 2θ of ~8°, which corresponded to the weak diffraction with a 2θ of 7.9° in the 1D WAXD patterns, appeared to be ring-like or arc-like in Figure 5a. Therefore, it might be attributed to the lateral packing of the polymer, possibly to the lateral periodic arrangement of aromatic units of the side groups. This weak diffraction was not observed in Figure 5b, probably due to the smaller *Y* dimension compared with the *X* dimension of the film. For PCbzG2, when the X-ray incident beam was parallel to the shear direction, only a close-to-ring pattern was observed in the low-angle region (Figure 5d). When the X-ray incident beam was along *Y* (Figure 5e) and *Z* (Figure 5f) directions (both perpendicular to the shear direction), the patterns were similar. A pair of low-angle diffraction arcs with a *d*-spacing of 4.07 nm appeared on the median in addition to a diffuse high-angle halo concentrated on the equator (Figure 5e,f). The low-angle ring pattern in Figure 5d and the resemblance of the patterns in Figures 5e and 5f confirmed the existence of a columnar phase instead of a smectic phase. Although it was still difficult to determine the exact phase structure due to limited diffractions, the phase of PCbzG2 could be a columnar nematic phase, Φ_N (Figure 6b). The columnar diameter of PCbzG2 was 4.07 nm, also quite close to the simulated molecular length (3.88 nm) of **monomer 2**. The different phase structures of the two polymers might originate from the different degrees of polymerization. PCbzG1 had a higher MW than PCbzG2 (Table 1). However, the columnar diameter of PCbzG1 was smaller than that of PCbzG2. Therefore, the aspect ratio (L/D) of PCbzG1 was larger than that of PCbzG2 (Figure 6) so that PCbzG1 was prone to form a more ordered structure.

For side-chain-type electroluminescent polymers, the main chain tend to take a coil-like conformation. Most of

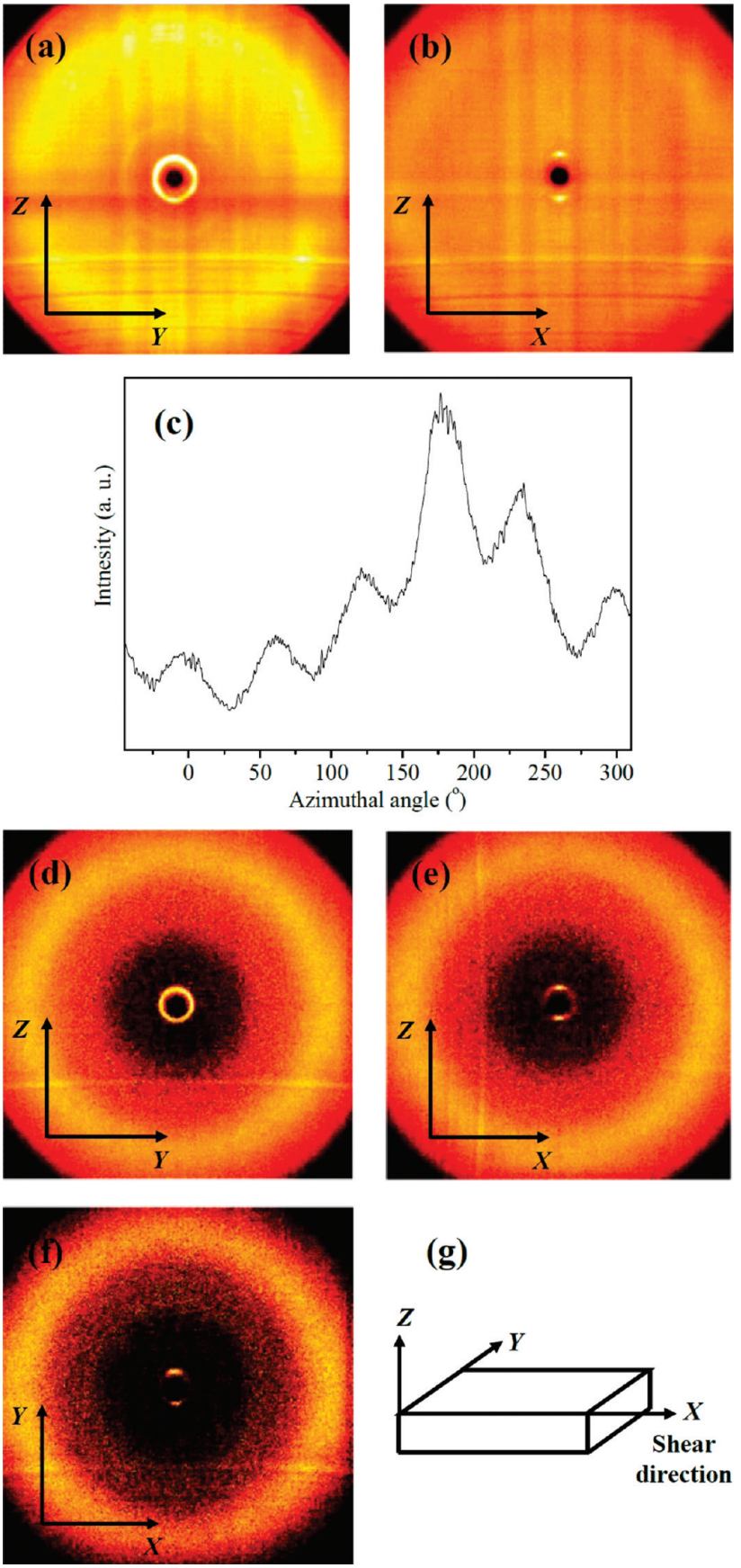

Figure 5. 2D WAXD patterns of PCbzG1 (a and b) and PCbzG2 (d, e, and f) with the X-ray incident beam parallel (a and d) and perpendicular (b, e, and f) to the shear direction; azimuthal scan of (a) for $2\theta = 2-3°$ (c); schematic drawing of the shearing geometry with X-axis the shear direction (g).

the functional side groups are wrapped into the coil and can easily interact with one another. For the dendronized jacketed polymers in this work, when the supramolecular columns formed, the jacketed main chain extended into a rod-like

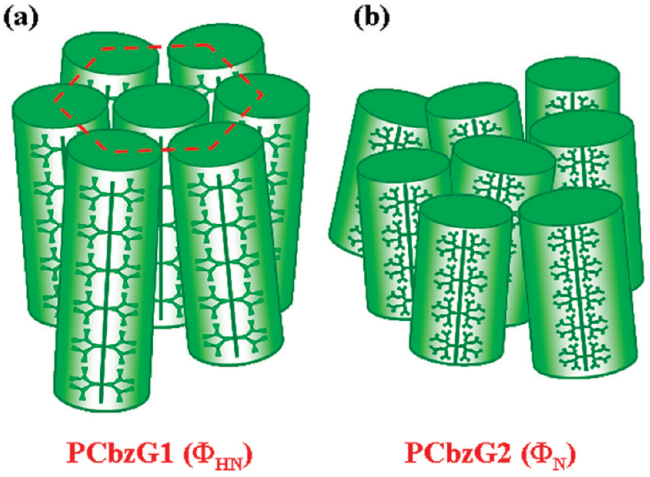

Figure 6. Schematic illustrations of the hexatic columnar nematic phase of PCbzG1 (a) and the columnar nematic phase of PCbzG2 (b).

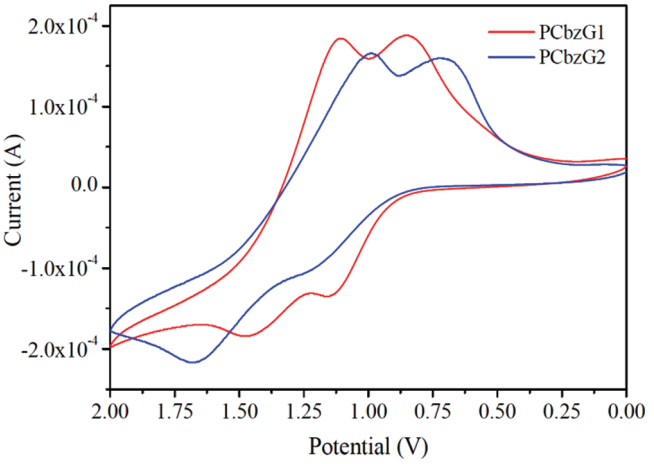

Figure 7. Cyclic voltammograms of the dendronized polymer films coated on the carbon electrode.

conformation, and all the functional groups were distributed on the surface of the column. This stiff main-chain structure and the dendritic side-group structure could reduce the intramolecular interactions and aggregations of the functional groups and prevent the formation of excimers, which would be beneficial to the photophysical properties.

Electrochemical Properties. In order to investigate the electrochemical properties of the dendronized polymers, cyclic voltammetry (CV) was utilized. The results are illustrated in Figure 7. As carbazoles and their derivatives are usually electron-rich systems, it was difficult to obtain the reduction information from the CV test, and we could only find the oxidation peaks in the CV curves. The HOMO levels of the dendronized polymers were estimated from the onset oxidation potentials by the equation $E_{HOMO} = -e[U_{onset(ox)} + (4.8\ V - U_{1/2,FOC})]$. Since the reduction peaks could not be obtained, we used the optical band gap (E_g) to estimate the LUMO levels by the equation $E_{LUMO} = E_{HOMO} + E_g$, where E_g was calculated from the onset absorbing wavelength in the UV−vis spectra in films. The detailed data are summarized in Table 3.

As shown in Figure 7 and Table 3, the two polymers exhibited similar electrochemical properties. This could be attributed to the jacketed structures of the polymers. The carbazole units were all attached on the surface of the cylindrical polymer chains, which made the carbazoles much

Table 3. Electrochemical Properties of the Dendronized Polymers

polymer	λ_{edge} (nm)[a]	E_g (eV)[b]	$U_{onset(ox)}$ (V)[c]	E_{HOMO} (eV)	E_{LUMO} (eV)
PCbzG1	358	3.46	0.91	−5.26	−1.80
PCbzG2	357	3.47	0.90	−5.25	−1.78

[a] The onset value of absorption spectrum in the long-wavelength range. [b] Estimated from the formula $E_g = 1240/\lambda_{edge}$. [c] Measured by cyclic voltammetry.

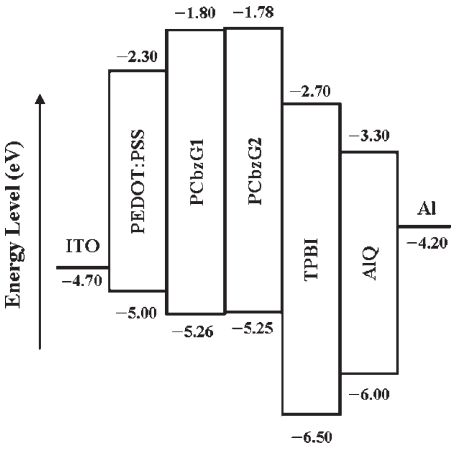

Figure 8. Energy level diagram of the materials used in this study.

easier to lose electrons. Changing the generation of the polymer only resulted in a different diameter of the cylindrical structure, and it had little effect on the electron receiving or losing properties. Therefore, both the polymers had high HOMO levels that were quite close to that of PEDOT:PSS (Figure 8), which suggested that they were very suitable for transporting of holes.

Electroluminescent Properties. The electroluminescent devices were fabricated in two configurations (device **a**, ITO/PEDOT:PSS/sample/TPBI(15 nm)/LiF(1 nm)/Al(100 nm); device **b**, ITO/PEDOT:PSS/sample/TPBI(15 nm)/AlQ(30 nm)/LiF(1 nm)/Al(100 nm)). In order to investigate the light-emitting properties of the target polymers with dendronized carbazole units, a hole-blocking layer was introduced into the devices to inhibit the formation of excitons near the electrode. TPBI has a lower HOMO level and thus possesses excellent hole-blocking properties. Therefore, it was chosen in this study. For device **b**, when the TPBI layer was removed, excitons formed in the AlQ layer, and we obtained the green emission from AlQ rather than the blue emission from the polymers. The electroluminescent spectra of devices **a** were collected at 6 V, and the two polymers exhibited similar EL behavior with the main emission peaks at around 435 and 488 nm (Figure 9). With increasing number of generation of dendrons, little difference was observed between the two EL spectra. Compared with PL spectra, the main emission peak only red-shifted 5−8 nm, which indicated that similar excited-state structures formed in both optic and electronic exciting processes. A new shoulder emission appeared at a longer wavelength, probably due to the formation of a new molecular exciting state under the electric field.

The properties of the devices are summarized in Table 4. The luminous efficiency (η_L) vs voltage curves and external quantum efficiency (η_{ext}) vs voltage curves are shown in Figure 10. All the devices could be turned on at a low voltage of no more than 6.1 V. These voltages were even lower than those of devices made from our previously reported jacketed polymers.[22,24,26] This was probably due to the good hole-transporting properties of the carbazole

units, especially when the carbazoles were grafted onto the surfaces of the cylindrical polymer chains, which might result in the formation of a continuous carrier-transporting channel. In addition, the better matching of the HOMO levels also contributed to the lower turn-on voltages.

Although a hole-blocking layer had been introduced into the devices to confine the holes in the emitting layer, the current efficiencies of devices **a** were quite low, which indicated the existence of a current leakage and a low electro-optic conversion efficiency. In order to reduce the current leakage, a better balance between the electron transport and hole transport was important. Therefore, in devices **b**, an electron-transporting layer (AlQ) was incorporated, resulting in greatly improved devices properties. Device **b** with PCbzG1 had the best comprehensive properties. The maximum luminescence was 2195 cd/m^2, and the maximum external quantum efficiency was 0.353%, with both values 4 times higher than those of device **a**. The maximum current efficiency and the power efficiency were 0.240 cd/A and 0.110 lm/W, respectively, both of which were 2 times higher than those of device **a**. These data were better than those obtained with the jacketed polymers we reported previously.[22,26] The turn-on voltages of devices **b** were a little higher than those of devices **a**, which was due to the incorporation of an additional AlQ layer. These results could be explained from the energy level diagram in Figure 8. In device **a**, electrons were injected from the Al cathode directly to the TPBI layer, in which process an energy barrier of 1.5 eV needed to be overcome. When an AlQ layer was introduced into the device, the energy barrier went down to 0.9 eV, which greatly increased the injection and transport of electrons and thus greatly improved the balance of the carrier transport. The better EL properties of PCbzG1 than PCbzG2 in both device configurations were probably due to the introduction of more nonfunctional components into **monomer 2**.

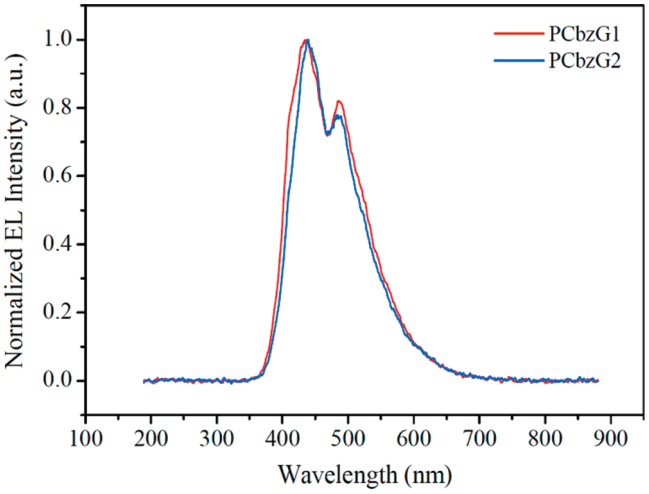

Figure 9. Electroluminescent spectra of devices **a**.

Conclusions

In summary, jacketed polymers with the first- and second-generation carbazole dendrons were synthesized by a "graft through" strategy. The second-generation polymer had a lower apparent molecular weight and a lower yield than those of the first-generation polymer. The glass transition temperatures and the 5% weight loss temperatures of the two polymers were about 85 and 360 °C, respectively. Their photophysical properties were similar in different solvents. The PL spectra in films blue-shifted 10 nm compared with those in solutions. After the films were annealed, the emission peaks in PL spectra became narrower, which was probably due to the transition of the chain conformation. X-ray diffraction experiments revealed that the first-generation polymer formed a hexatic columnar nematic phase and the second-generation polymer formed a columnar nematic phase. Electrochemical studies showed that the HOMO levels of the two polymers were quite high and close to that of PEDOT:PSS, which suggested that they possessed excellent hole-transporting properties. All the EL devices possessed low turn-on

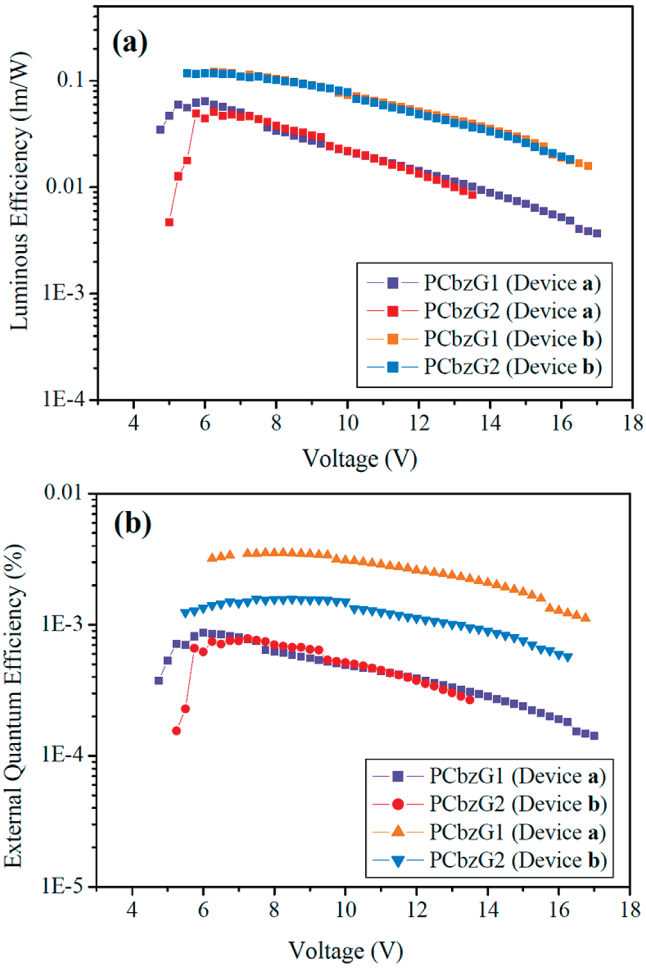

Figure 10. Luminous efficiency−voltage (a) and external quantum efficiency−voltage (b) curves for the devices with different polymers.

Table 4. Electroluminescent Properties of the Dendronized Polymers

device	polymer	V_{onset} (V)[a]	L_{max} (cd/m^2)[b]	η_{Imax} (cd/A)[c]	η_{Lmax} (lm/W)[d]	η_{extmax} (%)[e]	CIE coordinate[f]	λ (nm)[g]
a	PCbzG1	4.6	555	0.110	0.056	0.087	(0.18, 0.16)	428, 483
a	PCbzG2	5.1	327	0.107	0.051	0.078		
b	PCbzG1	6.1	2195	0.240	0.110	0.353	(0.18, 0.20)	434, 487
b	PCbzG2	5.3	1796	0.236	0.106	0.158	(0.19, 0.22)	439, 488

[a] Turn-on voltage at 1 cd/m^2. [b] Maximum luminance. [c] Maximum current efficiency. [d] Maximum luminescence efficiency. [e] Maximum external quantum efficiency. [f] 1931 CIE coordinate. [g] Emission wavelength at 6 V.

voltages compared with those having some other side-chain-type EL polymers. After the optimization of the device structure, device **b** with PCbzG1 obtained the best performance. The maximum luminescence, current efficiency, and external quantum efficiency were 2195 cd/m^2, 0.240 cd/A, and 0.353%, respectively. The comprehensive properties were better than those of the devices with the jacketed polymers we reported previously because the novel dendronized jacketed structure could reduce the intramolecular interactions of functional groups, make full use of the large surfaces of the supramolecular columns, and provide a continuous channel for transporting of holes. With increasing number of generation of the dendrons, the EL properties became worse due to the decrease in the content of functional units. Currently we are investigating the controlled/living polymerization of the two dendronized monomers and the applications of these new jacketed polymers as host materials for electrophosphorescent devices.

Acknowledgment. Financial support from the National Natural Science Foundation of China (Grant Nos.: 20634010, 20974002, and 20990232) is gratefully acknowledged.

References and Notes

(1) Tang, C. W.; VanSlyke, S. A. *Appl. Phys. Lett*. **1987**, *51*, 913–915.
(2) Veinot, J. G. C.; Marks, T. J. *Acc. Chem. Res*. **2005**, *38*, 632–643.
(3) Burn, P. L.; Lo, S.-C.; Samuel, I. *Adv. Mater*. **2007**, *19*, 1675–1688.
(4) Hwang, S.-H.; Moorefield, C. N.; Newkome, G. R. *Chem. Soc. Rev*. **2008**, *37*, 2543–2557.
(5) Burroughes, J. H.; Bradley, D. D. C.; Brown, A. R.; Marks, R. N.; Mackay, K.; Friend, R. H.; Burns, P. L.; Holmes, A. B. *Nature* **1990**, *347*, 539–541.
(6) Yeh, K.-M.; Chen, Y. *J. Polym. Sci., Part A: Polym. Chem*. **2007**, *45*, 2259–2272.
(7) Zhang, K.; Tao, Y.; Yang, C.; You, H.; Zou, Y.; Qin, J.; Ma, D. *Chem. Mater*. **2008**, *20*, 7324–7331.
(8) Wu, C.-W.; Lin, H.-C. *Macromolecules* **2006**, *39*, 7232–7240.
(9) Chi, J. H.; Park, S. H.; Lee, C.-L.; Kim, J. J.; Jung, J. C. *Macromol. Mater. Eng*. **2007**, *292*, 844–854.
(10) Grisorio, R.; Mastrorilli, P.; Nobile, C. F.; Romanazzi, G.; Suranna, G. P.; Gigli, G.; Piliego, C.; Ciccarella, G.; Cosma, P.; Acierno, D.; Amendola, E. *Macromolecules* **2007**, *40*, 4865–4873.
(11) Yeh, K.-M.; Chen, Y. *J. Polym. Sci., Part A: Polym. Chem*. **2006**, *44*, 5362–5377.
(12) You, Y.; Kim, S. H.; Jung, H. K.; Park, S. Y. *Macromolecules* **2006**, *39*, 349–356.
(13) Tokito, S.; Suzuki, M.; Sato, F.; Kamachi, M.; Shirane, K. *Org. Electron*. **2003**, *4*, 105–111.
(14) Ma, B.; Kim, B. J.; Deng, L.; Poulsen, D. A.; Thompson, M. E.; Frechet, J. M. J. *Macromolecules* **2007**, *40*, 8156–8161.
(15) Furuta, P. Y.; Deng, L.; Garon, S.; Thompson, M. E.; Fréchet, J. M. J. *J. Am. Chem. Soc*. **2004**, *126*, 15388–15389.
(16) Zhao, P.; Ling, Q.-D.; Wang, W.-Z.; Ru, J.; Li, S.-B.; Huang, W. *J. Polym. Sci., Part A: Polym. Chem*. **2007**, *45*, 242–252.
(17) Tao, Y.; Ma, B.; Segalman, R. A. *Macromolecules* **2008**, *41*, 7152–7159.
(18) Zhou, Q. F.; Li, H. M.; Feng, X. D. *Macromolecules* **1987**, *20*, 233–234.
(19) Zhou, Q.; Zhu, X.; Wen, Z. *Macromolecules* **1989**, *22*, 491–493.
(20) Gao, L.-C.; Fan, X.-H.; Shen, Z.-H.; Chen, X.; Zhou, Q.-F. *J. Polym. Sci., Part A: Polym. Chem*. **2009**, *47*, 319–330.
(21) Chen, X.-F.; Shen, Z.; Wan, X.-H.; Fan, X.-H.; Chen, E.-Q.; Ma, Y.; Zhou, Q.-F. *Chem. Soc. Rev*. **2010**, *39*, 3072–3101.
(22) Wang, P.; Chai, C.; Wang, F.; Chuai, Y.; Chen, X.; Fan, X.; Zou, D.; Zhou, Q. *J. Polym. Sci., Part A: Polym. Chem*. **2008**, *46*, 1843–1851.
(23) Wang, P.; Jin, H.; Yang, Q.; Liu, W.; Shen, Z.; Chen, X.; Fan, X.; Zou, D.; Zhou, Q. *J. Polym. Sci., Part A: Polym. Chem*. **2009**, *47*, 4555–4565.
(24) Wang, P.; Yang, Q.; Jin, H.; Liu, W.; Shen, Z.; Chen, X.; Fan, X.; Zou, D.; Zhou, Q. *Macromolecules* **2008**, *41*, 8354–8359.
(25) Yang, Q.; Jin, H.; Xu, Y.; Wang, P.; Liang, X.; Shen, Z.; Chen, X.; Zou, D.; Fan, X.; Zhou, Q. *Macromolecules* **2009**, *42*, 1037–1046.
(26) Yang, Q.; Xu, Y.; Jin, H.; Shen, Z.; Chen, X.; Zou, D.; Fan, X.; Zhou, Q. *J. Polym. Sci., Part A: Polym. Chem*. **2009**, *48*, 1502–1515.
(27) Rosen, B. M.; Wilson, C. J.; Wilson, D. A.; Peterca, M.; Imam, M. R.; Percec, V. *Chem. Rev*. **2009**, *109*, 6275–6540.
(28) Rudick, J. G.; Percec, V. *Acc. Chem. Res*. **2008**, *41*, 1641–1652.
(29) Percec, V.; Ahn, C. H.; Ungar, G.; Yeardley, D. J. P.; Moller, M.; Sheiko, S. S. *Nature* **1998**, *391*, 161–164.
(30) Zhang, A.; Shu, L.; Bo, Z.; Schluer, A. D. *Macromol. Chem. Phys*. **2003**, *204*, 328–339.
(31) Percec, V.; Ahn, C. H.; Cho, W. D.; Jamieson, A. M.; Kim, J.; Leman, T.; Schmidt, M.; Gerle, M.; Moller, M.; Prokhorova, S. A.; Sheiko, S. S.; Cheng, S. Z. D.; Zhang, A.; Ungar, G.; Yeardley, D. J. P. *J. Am. Chem. Soc*. **1998**, *120*, 8619–8631.
(32) Prokhorova, S. A.; Sheiko, S. S.; Möller, M.; Ahn, C. H.; Percec, V. *Macromol. Rapid Commun*. **1998**, *19*, 359–366.
(33) Percec, V.; Obata, M.; Rudick, J. G.; De, B. B.; Glodde, M.; Bera, T. K.; Magonov, S. N.; Balagurusamy, V. S. K.; Heiney, P. A. **2002**, *40*, 3509−3533.
(34) Schluer, A. D.; Rabe, J. P. *Angew. Chem., Int. Ed*. **2000**, *39*, 864–883.
(35) Helms, B.; Mynar, J. L.; Hawker, C. J.; Frechet, J. M. J. *J. Am. Chem. Soc*. **2004**, *126*, 15020–15021.
(36) Sheiko, S. S.; Sumerlin, B. S.; Matyjaszewski, K. *Prog. Polym. Sci*. **2008**, *33*, 759–785.
(37) Peng, Q.; Xu, J.; Li, M.; Zheng, W. *Macromolecules* **2009**, *42*, 5478–5485.
(38) Setayesh, S.; Grimsdale, A. C.; Weil, T.; Enkelmann, V.; Mullen, K.; Meghdadi, F.; List, E. J. W.; Leising, G. *J. Am. Chem. Soc*. **2001**, *123*, 946–953.
(39) Peng, Q.; Li, M.; Lu, S.; Tang, X. *Macromol. Rapid Commun*. **2007**, *28*, 785–791.
(40) Yuan, M.-C.; Shih, P.-I.; Chien, C.-H.; Shu, C.-F. *J. Polym. Sci., Part A: Polym. Chem*. **2007**, *45*, 2925–2937.
(41) Tomalia, D. A. *Soft Matter* **2010**, *6*, 456–474.
(42) Zheng, Y.; Zhou, Y.; Accorsi, G.; Armaroli, N. *J. Rare Earths* **2008**, *26*, 173–177.